CrossMark

ORIGINAL PAPER

Simultaneous detection of multiple viruses in their co-infected cells using multicolour imaging with self-assembled quantum dot probes

Thaer Kadhim Fayyadh [1,2,3] · Fuying Ma [1] · Chong Qin [2] · Xiaowei Zhang [2] · Wei Li [2] ·
Xian-En Zhang [4] · Zhiping Zhang [2] · Zongqiang Cui [2]

Abstract The simultaneous detection and evaluation of the coinfection of a cell by multiple viruses or even multiple subtypes still is a difficult challenge. The authors introduce a method for simultaneous imaging, detection and quantitative evaluation of multiple viruses in single cells by using multicolor quantum dot (QD) probes and in a single staining cycle. The multicolor QD probes were fabricated via interaction between QDs conjugated to *Staph. aureus* protein A (SpA-QDs) and virus-specific antibodies. A cocktail of differently colored QD-SpA-MAbs probes were loaded into the same cells containing multiple viruses, and this enabled the different viruses to be fluorescently imaged and analyzed simultaneously. Specifically, influenza A viruses of type H1N1, H3N2, and H9N2, as well as human adenovirus species B type 3 (HAdV-B3) were imaged and detected in virus-infected cells or in their co-infected cells. In our perception, the method provides a flexible platform for simultaneous detection of multiple viruses in co-infected cells. Hence, it offers new opportunities for the molecular diagnosis of virus coinfection and for studies on virus-cell interactions.

Keywords Coinfection detection · Multiple viruses · SpA-QDs · Influenza a virus · Human adenovirus

Introduction

Virus coinfection is frequently observed in clinical settings [1, 2]. The simultaneous detection and quantitative evaluation of the coinfection of a cell by multiple viruses or even multiple subtypes is urgently in demand, yet it remains difficult. Several laboratory methods are available for detecting viruses, but they have disadvantages for the simultaneous detection and quantitative evaluation of multiple viruses in a single cell. Currently available multiplex PCR methods have been widely used for the detection of multiple viruses [3]. However, they require a marker of a professional primer and carefully designed probes to avoid cross- and mis-hybridization [4]. More importantly, with PCR-based methods as well as some other methods, including gene chips, two-dimensional gel electrophoresis, and biomolecular mass spectrometry, it is difficult to provide the subcellular localization information and single-cell analysis results for the different co-infecting viruses [1, 5]. The direct isolation and culture of viruses in cell lines is a convincing method and the gold standard, but it requires skilled technologists and specialized laboratory settings as well as a long turnaround time [6]. In addition, many viruses cannot be covered by culture. Immunofluorescence (IF) by labelling antibodies with fluorophores is available for virus detection in single cells. However, such probes have been limited to the qualitative evaluation of 2–3 colours in most cases and relatively low sensitivity due to the unfavourable optical properties of organic dyes [7].

Thaer Kadhim Fayyadh and Fuying Ma contributed equally to this work

✉ Zongqiang Cui
czq@wh.iov.cn

1   College of Life Science and Technology, Huazhong University of Science and Technology, Wuhan, People's Republic of China

2   State Key Laboratory of Virology, Wuhan Institute of Virology, Chinese Academy of Sciences, Wuhan, People's Republic of China

3   Ministry of Health (MOH), Baghdad, Iraq

4   National Laboratory of Biomacromolecules, CAS Center for Excellence in Biomacromolecules, Institute of Biophysics, Chinese Academy of Sciences, Beijing, People's Republic of China

Alternatively, in comparison with organic dyes, quantum dots (QDs) have good optical properties; including size-tuneable light emission, improved signal brightness, resistance against photobleaching and the simultaneous excitation of multiple fluorescence colours [8]. Compared to other fluorescent nanoparticles such as carbon dots or upconversion nanoparticles, QDs have higher photo-quantum efficiency and more colours. Based on these good optical properties, QD-based methods have been built for biomolecular and virus detection. In particular, comprehensive molecular profiling of individual cells has been achieved by using QDs [9].

In this study, by using the multicolour QD-probes and a single staining procedure cycle, we have realized the simultaneous detection and quantitative evaluation of multiple viruses in their infected cells. Multicolour QD-probes were efficiently fabricated via self-assembly between *Staph aureus* protein A conjugated-QDs (SpA-QDs) and virus-specific antibodies. We have acquired multicolour QD-probes for the influenza A viruses H1N1, H3N2 and H9N2 as well as HAdV-B3 by using this rapid and self-assembly probe preparation process without purification. Multiple viruses in the same cell can be simultaneously imaged and analysed after a single staining cycle. Several different influenza virus subtypes and HAdV-B3 virus were detected and quantitatively evaluated in their co-infected cells.

Materials and methods

Materials and reagents

Core/shell CdSe/ ZnS QDs with emission peaks centred at 525, 625 and 705 were purchased from Wuhan Jiayuan Quantum Dots Co. Ltd. (China, www.qds.net.cn), and conjugated with protein A due to the action of the coupling agent 1-ethyl-3-(3-dimethylaminopropyl) carbodiimide hydrochloride (EDC). Mouse-MAb to influenza A H1N1, H3N2 and H9N2 hemagglutinin (HA) were purchased from Sino Biological Inc., (China, www.sinobiological.com). Alexa Fluor® 488 goat anti-mouse IgG was purchased from Cell Signalling Technology (USA, www.cellsignal.com), whereas mouse-MAb anti-adenovirus was from Abcam, (UK, www.abcam.com). Other reagents included the following: Dulbecco's Modified Eagle's Medium (DMEM), foetal bovine serum (FBS), trypsin-EDTA, 0.25% solution, penicillin-streptomycin 10,000 U/ mL and Dulbecco's phosphate buffered saline (DPBS) modified without Ca^{2+} and Mg^{2+}, from GE healthcare life science (USA, www.gelifesciences.com); 16% formaldehyde solution (methanol-free solution), IgG elution buffer (pH = 2.8), and Triton X-100 in H_2O from Thermo Scientific, (USA, www.thermoscientific.com); dodecyltrimethyl-ammonium chloride (DTAC), sodium dodecyl sulphate (SDS) and bovine serum albumin (BSA) Sigma-Aldrich (USA, www.sigmaaldrich.com); and 5% (wt/vol) casein (alkali-soluble) Novagen, (Germany, www.novagen.com); Hoechst 33,342, from Beyotime Biotechnology (China, www.beyotime.com).

Cell lines and viruses

Madin–Darby canine kidney (MDCK) and human bronchial epithelial (A549) cells were cultivated in DMEM with 10% FBS at 37 °C in a 5% CO_2 atmosphere. Influenza A virus subtypes used included (H1N1)A/Puerto Rico/8/1934(PR8), A/H9N2 strain A/chicken/Jiangsu/7/2002(Jia02), seasonal influenza A/H3N2 strain A /Human / Ningb/2009 (Hub05), and HAdV-B3 was also used. Viruses were kindly provided from the Wuhan Institute of Virology, Chinese Academy of Sciences. After being propagated in the allantoic cavity of 10-day-old embryonated eggs, H9N2, H1N1 and H3N2 viruses were purified by differential centrifugation and density gradient centrifugation as previously described [10].

Virus inoculation in 35 mm glass-bottom dishes

For single-cycle experiments, a confluent monolayer of MDCK or A549 cells was maintained in T-25 cm^2 flasks in cell growth medium (CGM) as described above, and then, the cells were cultivated in 35 mm glass-bottom dishes for virus inoculation. The inoculums were prepared by diluting the frozen stocks of viruses in infection medium (IM) [CGM without FBS and supplemented with TPCK-trypsin (2 μg /mL)] at a multiplicity of infection (MOI) of 10, and they were inoculated with 100 μL/dish of diluted virus onto the monolayer cells (for single or multiple subtypes of viruses). The cells were incubated at 4 °C for 10 min and then at 37 °C for 5 min in 5% CO_2 to allow viral adsorption or at 37 °C for different post infection time points (pi) of 4, 8, 16 and 24 h for the quantitative evaluation of the viruses. Subsequently, cells were washed twice with 1× TBS, fixed by 4% formaldehyde in TBS for 20 min at room temperature (RT), washed by 1 mL/dish of 1× TBS, permeabilized with 2% DTAC/TBS for 20 min followed by 0.25% Triton x-100/TBS for 5 min, and washed twice with 1 mL/dish of 1× TBS. Afterwards, the excess solution was discarded, and the cells were washed 3 times with 1 mL/dish of elution buffer with 0.5% (wt/vol) SDS as a regeneration buffer for 5 min. Thereafter, the dishes were rinsed with 1 mL/dish of 1× TBS, followed by blocking by 1 mL/dish of 2% (wt/vol) BSA, 0.1% (wt/vol) casein, and 1× TBS, and incubated at RT for 30 min.

Preparation of QD-SpA-MAb probes

To label one type of target HA protein (influenza viruses) or hexon protein (HAdV-B3) in one 35 mm glass-bottom dish by QD-SpA-MAb probes, bio-conjugation was carried out by

combining 2.5 μL of 1× PBS, 1.5 μL of 0.2 mg/mL MAbs and 6 μL of 1 μM QD-SpA in a separate 150-μL microcentrifuge tube with mixing by pipetting, followed by incubation for 1 h at RT as previously described [9].

Transmission electron microscopy (TEM) analysis

For TEM analysis, carbon-coated copper grids were laid on drops containing 0.5 mg/ mL QD-SpA and QD-SpA-MAb for 2 min. After removal of the redundant liquid using filter paper and washing with MilliQ water, all samples were negatively stained with 2% phosphotungstic acid (PTA) for 2 min and subsequently examined under a Hitachi H7000 TEM.

Dynamic light scattering

The size of QD-SpA-MAb was characterized using dynamic light scattering (DLS). DLS measurements were performed on a NanoZS 90 Zetasizer instrument (Malvern, UK) as previously described [11].

Labelling target proteins by QD-SpA-MAb probes

Briefly, in 1, 2, or 3 separate 1.5 mL tubes (depending on the numbers of targets), 10 μL of QD-SpA-MAb complex was diluted to 300 μL with 6% (wt/vol) BSA in 1× TBS as staining buffer for the infected dishes and control, respectively. The blocking buffer was removed and replaced in infected dishes and the control with 300 μL/dish of diluted QD-SpA-MAb. The treated dishes were incubated at RT for 2 h in a dark place. The final washing was performed for 10 min once with 1 mL/ dish of 1% (wt/vol) BSA, 0.1% (wt/vol) casein, and 1× TBS as a washing buffer, and then the dish was washed twice for 5 min with 1 mL/dish of 1× TBS. Nucleus staining was performed with additional Hoechst 33,258 stain. Thereafter, cells were immersed in 1 mL of 1× TBS, and the images were acquired for analysis under a confocal microscope system. The traditional IF assays were carried out as shown in the supplementary Materials and Methods.

Fluorescence imaging and analysis

Fluorescence was imaged with an UltraView Vox spinning disk confocal laser scanning system (PerkinElmer, Co.) using a Nikon Ti-e microscope (Japan) with a 60× objective lens. QD525,QD625 and QD705 were excited with 488-nm, 561-nm, 640-nm lasers and detected with 525-nm (W50), 615-nm (W70), 705-nm (W90) nm emission filter respectively. Fluorescence analysis was carried out by using Volocity software.

Results and discussion

Protocol design of the multicolour QD imaging for the simultaneous detection of multiple viruses

As schematically illustrated in Fig. 1a, QDs were first covalently linked with SpA (step 1). This bio-conjugation is most commonly based on cross-linking reactions between amine and carboxylic acid groups (catalysed by carbodiimide) [12]. Then, the QD-SpA conjugates captured free MAbs in the solution via self-assembly, with SpA acting as an adaptor for the orientation-controlled IgG immobilization via binding to the Fc region of IgG (step 2). When the molar ratio of SpA to IgG is relatively high, all the MAbs will be conjugated with the QD-SpA, and after the formation of the QD-SpA-MAb complex, there are no sterically accessible binding sites left on the MAb, which prevents cross-linking of different QDs via MAbs [13, 14]. This ensured that the QD-SpA-MAb probe preparation did not require a probe purification process [15]. The formation of different functional QD-SpA-MAb probes either are pooled in one coloured complex cocktail or kept separate with a single probe for each one (step 3). These probes will target their own specific target of interest (step 4).

### Construction and characterization of the QD-SpA-MAb probes

Here, QDs 525, 625 and 705 decorated by the PEG of carboxyl groups and labelled with protein A conjugates were first incubated with H1N1 HA MAbs to create fully self-assembled probes. The probe complexes of QD-SpA conjugated with H1N1 HA MAbs, and QD625-SpA-MAb, QD705-SpA-MAb and QD525-SpA-MAb probes were fabricated and characterized. The DLS analysis (Fig. 1b) shows that the hydro- dynamic.

Sizes of QD625-SpA, QD705-SpA and QD525-SpA before conjugation are approximately 18, 12 and 18 nm, and this size increased to approximately 28, 20 and 20 nm, respectively, after conjugation with the antibodies. TEM images also show that the QD-SpA-MAb probes presented a narrow size distribution and high mono-disparity with average sizes of approximately 10–15, 12–17 and 10–15 nm, respectively (Fig. 1c). From these measurements, we conclude the successful bio-conjugation of MAbs with QD-SpA, and this observation is consistent with a recently published report by Feng Wu and colleagues [16].

QD-SpA-MAb probes were tested for virus detection in virus infected cells

Then, the QD-SpA-MAb probes were tested for virus detection in cells. As shown in Fig. 2a, there is obvious QD fluorescent signal in the cells infected with H1N1 virus incubated with fully assembly QD625-SpA-MAb as a "one-step procedure". When the infected cells were first incubated with

Fig. 1 Protocol design of the QD-SpA-MAb probes for the detection and characterization of multiple viruses. **a** Schematic illustration of the construction of the probes and simultaneous labelling of multiple viruses. QDs were covalently linked with SpA (step 1). QD-SpA conjugates self-assembled with MAbs, and QD-SpA-MAb probes were acquired through a single-step purification-free procedure (step 2). Different coloured QD-SpA-MAb probes were mixed as a single cocktail (step 3). The QD-SpA-MAb cocktail was used for the simultaneous labelling of multiple viruses in their co-infected cells (step 4). **b** DLS analysis of QD-SpA and MAb-functionalized QD-SpA. QD625-SpA-MAb, QD705-SpA-MAb and QD525-SpA-MAb were analysed, respectively. **c** TEM images of different QD-SpA and MAb-functionalized QD-SpA
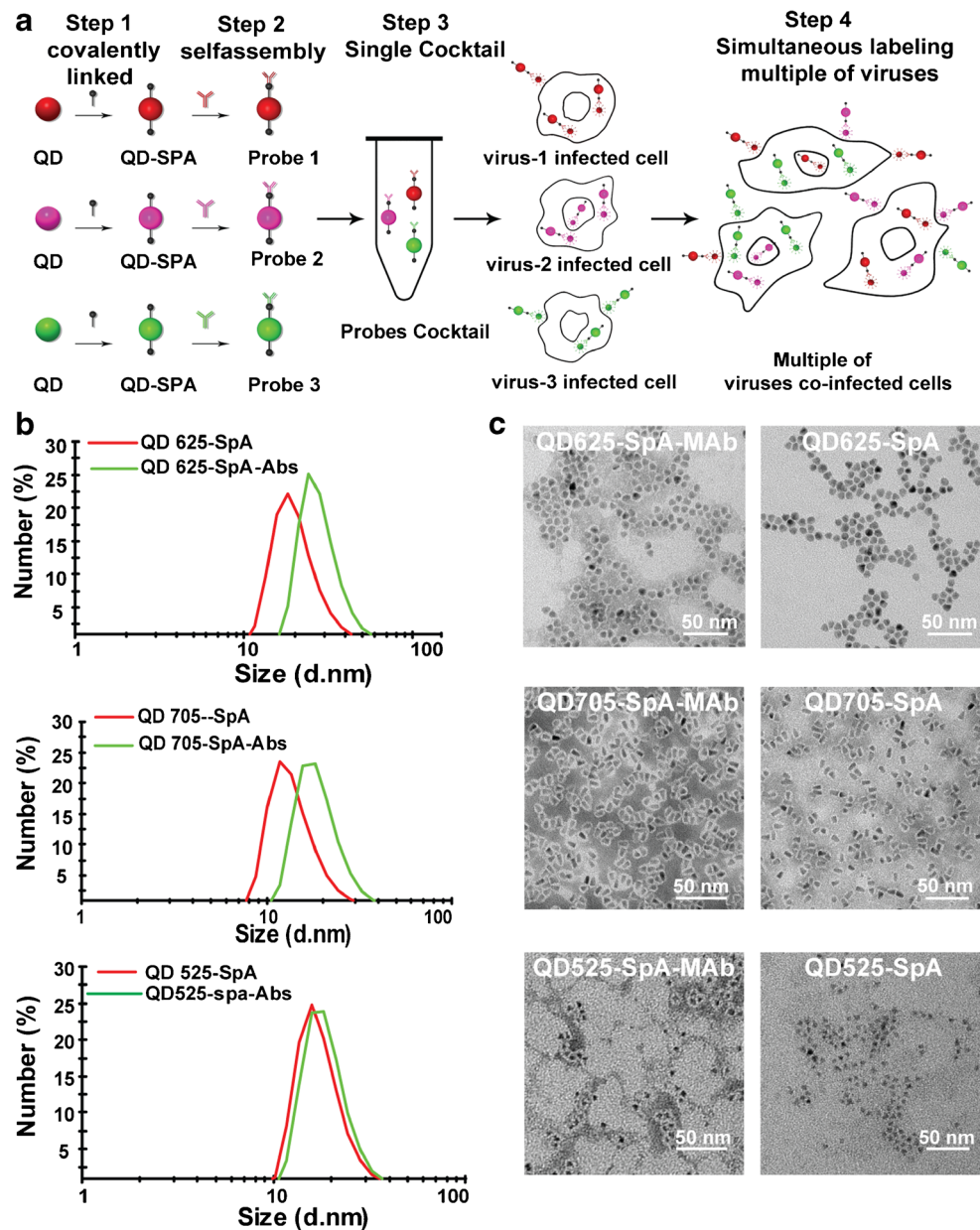

MAbs and then treated with the QD625-SpA complex as a "two-step procedure", a consistent labelling was also obtained (Fig. 2b). There was no signal in the non-infected cells. There was also no signal when the virus infected cells were treated with only the QD625-SpA complex.

The specific targeting of the QD-SpA-MAb probes was also verified by traditional IF. In the virus-infected cells with traditional IF signals from the MAbs and Alexa Fluor 488-labelled goat anti-mouse IgG 2′Ab, the QD625-SpA-MAb probes also show specific fluorescence. The QD signals were co-localized with traditional IF fluorescence from Alexa Fluor 488 (supplementary Fig. S1).

The self-assembly between QD-SpA and MAb means that there are no sterically accessible binding sites left on

Ab after QD–Ab complex formation, which prevents the cross-linking of different QD-SpA-MAb [17]. We also investigated whether cross-linking occurs during labelling. Here, before labelling, we mixed fully assembled QD-SpA-MAb probes with the counterpart QD-SpA complex (for example, QD625-SpA-MAb probe mixed with QD525-SpA complex, or vice versa) and incubated them with H1N1 virus-infected cells. Through this setup, if cross-linking exists, the excess of vacant counterpart QD-SpA complex would bind with any binding sites left on the Abs of the QD-SpA-MAb probes. The results display that there is no cross-linking or interference with QD625-SpA-MAb probes by QD525-SpA complex or vice versa because the QD525-SpA complex cannot bind to the QD625-Spa-
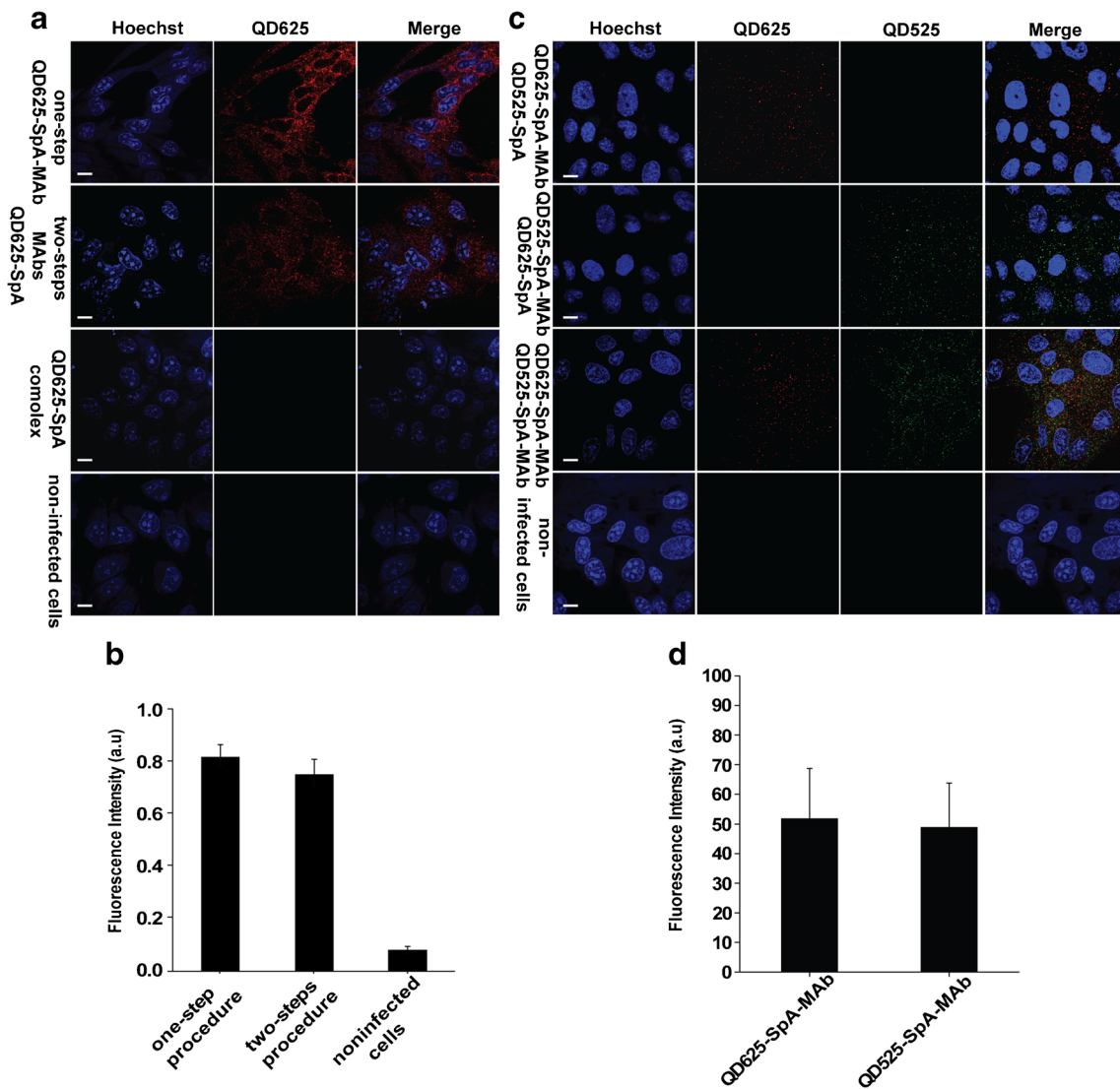
Fig. 2 Virus detection in cells with QD-SpA-MAb probes. **a** H1N1 virus was labelled in virus-infected MDCK cells with a "one-step procedure" by QD625-SpA-MAb or with a "two-step procedure" that was performed by first being incubated with MAbs and then with QD625-SpA. There was no signal when the virus-infected cells were treated with only QD625-SpA. There was also no signal in the non-infected cells. **b** Fluorescence intensities obtained from the labelling with one-step and two-steps procedures. **c** Cross-linking test of QD-SpA-MAb probes. The presence of a competitor QD525-SpA complex does not interfere with the target labelling by the fully assembled QD625-SpA-MAb probe during the labelling of H1N1 HA proteins. Similarly, the presence of the QD625-SpA complex does not interfere with target labelling by the QD525-SpA-MAb probe. When anti-HA MAb, QD525-SpA and QD625-SpA were mixed together and applied to infected cells, both of the QD525-SpA and QD625-SpA probes successfully capture MAbs and produce labelling signals. **d** Fluorescence quantification showed approximately 50% contributions for the QD525-SpA and QD625-SpA when they were mixed together with anti-HA MAb. Scale bar, 10 μm

MAb probe and the QD625-SpA complex cannot bind to the QD525-SpA-MAb probe (Fig. 2c). If QD525-SpA and QD625-SpA complexes are mixed simultaneously with MAbs and then incubated together with the same cells, they efficiently captured free MAbs from solution and produced mixed-colour HA labelling with approximately a 50% contribution from each probe (Fig. 2d). Analysis of Pearson correlation coefficient (0.97%) demonstrated the co-localization of QD525-SpA-MAb and QD625-SpA-MAb. In the non-infected cells, no red or green signals were found.

Our results support the conclusion that QD-SpA-MAb probes exhibit a lack of cross-linking and cross-talk. In our study, by incubating QD-SpA complexes in excess with MAbs before labelling, nearly the complete capture of MAbs by QD-SpA is expected, therefore preventing the binding of free MAbs to vacant SpA sites on different QD-SpA probes. SpA possesses five IgG-binding sites, two of which are simultaneously accessible [18], whereas IgG has two SpA-binding sites on its Fc region, making the formation of polymeric SpA-MAb complexes possible [17]. However, no

aggregation was observed between QD-SpA and MAbs by DLS, TEM, and fluorescence microscopy (Fig. 1). As demonstrated before, the potential divalent binding of both sites on the MAb by SpA bound to the QD surface, and the steric hindrance should offer a mechanism in preventing probe cross-linking [13].

Detection of different viruses using different specific QD-SpA-MAb probes Since our labelling strategy is suitable for virus detection in cells, we set out to detect different viral targets using QD-SpA-MAb probes. As shown in Fig. 3, H3N2 was detected in virus-infected MDCK cells by using the QD705-SpA-MAb targeting HA protein, and HAdV-B3 was detected in virus-infected A549 cell lines by using QD625-SpA-MAb probes targeting the hexon of HAdV-B3. The viruses can be detected at different post-infection time points and as early as 15 min after infection (Fig. 3a, b).

In our assay, the subcellular localization of the target of interest can also be clearly displayed. It is known that HA is located in the cytoplasm and along the cell surface [19]; therefore, the QD705-SpA-MAb probe targeted HA either along the cell surface or inside the cytoplasm (Fig. 3a). In contrast, the QD625-SpA-MAb probe targeting the hexon of HAdV-B3 showed a different subcellular distribution pattern from that for H1N1 at different post-infection time points. The QD signal targeting the hexon of HAdV-B3 was localized along the

cell surface and inside the cytoplasm during the early infection phase (15 min, 4 h) and concentrated mainly in the nucleus during the late infection phase (8 h, 16 h) (Fig. 3b). The HAdVs genome is transported into the nucleus, where viral gene transcription, viral DNA replication, and virion assembly occur [20]. Our observation is in agreement with the subcellular localization and functions of the hexon of HAdVs since the hexon plays roles in events occurring after internalization, such as transcriptional activation, and nuclear reorganization [20, 21]. These results from the detection of different viruses demonstrated that QD-SpA-MAb probes can be used to label different targets in different subcellular areas inside the cell.

Quantitative evaluation of viruses in cells by QD-SpA-MAb probes

QD-SpA-MAb probes were also tested for the quantitative evaluation of viruses in infected cells. Influenza A viruses H1N1 and H3N2 were detected at different time points (4, 8, 16 and 24 h pi) in their infected cells by QD625-SpA-MAb and QD525-SpA-MAb probes, respectively (Fig. 4a, supplementary Fig. S2). As shown in Fig. 4a, both viruses replicated efficiently in MDCK cells, as indicated by the marked increase in the IF intensity at early stages of infection. However, the H1N1 virus multiplication showed a steadier progressive logarithmic increase at the late stage of infection

Fig. 3 Detection of H3N2 in MDCK cells and HAdV-B3 in A549 cells (**a**) H3N2 virus was labelled with QD705-SpA-MAb probes targeting HA at different pi times. **b** HAdV-B3 virus was labelled with QD625-SpA-MAb probes targeting the hexon of HAdV-B3 at different pi times. Scale bar, 10 μm
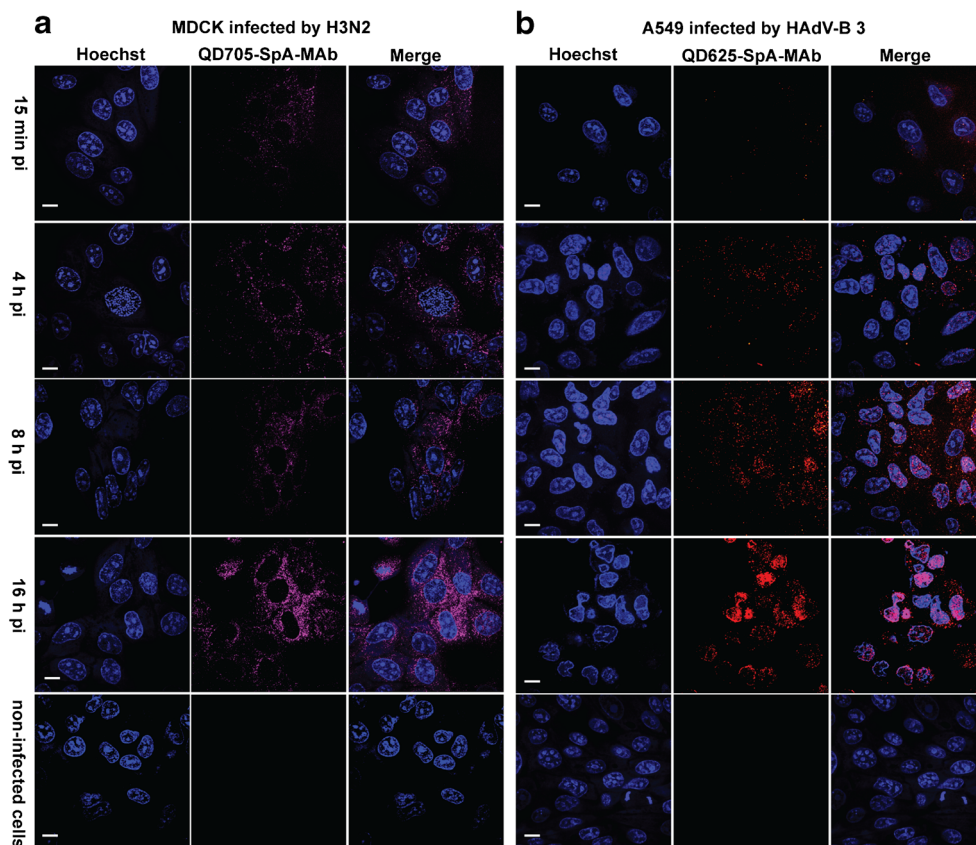
Fig. 4 Quantitative evaluations of H1N1 and H3N2 viruses at different pi time points (**a**) In single-virus infected cells, quantitative calculation of the fluorescence signals for H1N1 and H3N2 viruses at the indicated pi time points. **b** Quantitative evaluation of the virus proliferation for H1N1 and H3N2 viruses in their co-infected cells at the indicated pi time points
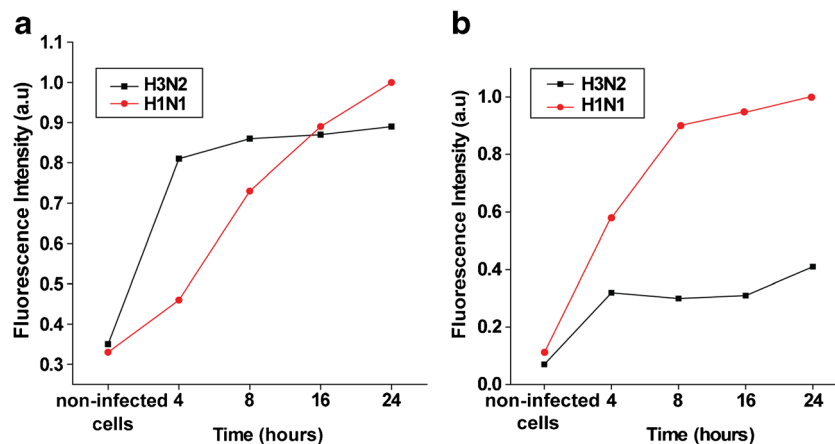
when compared with the H3N2 virus. Being similar to the influenza A viruses H1N1 and H3N2, HAdV-B3 was also quantitatively evaluated in A549 cells at different time points post- infection (supplementary Fig. S3).

We also quantitatively evaluated the co-infection of influenza A viruses H1N1 and H3N2 at different post-infection time points. As shown in Fig. 4b and supplementary Fig. S4, H1N1 and H3N2 viruses can be detected by QD625-SpA-MAb and QD525-SpA-MAb probes, respectively, in the same co-infected cells. Quantitative evaluation showed that both viruses replicated in their co-infected cells, but H3N2 virus replication had a lower quantity than that of the H1N1 virus (Fig. 4b). The results are in line with previously published works, which indicated that there were notable differences in the proliferation between the H1N1 and H3N2 subtypes, as demonstrated by the multiplex RT-PCR analysis of RNA extracted from the co-cultures of influenza H3N2 with H1N1 in MDCK cells [2]. Although both subtypes were able to infect MDCK cells initially, the coinfection of H1N1 and H3N2 would result in a decrease in the replication of H3N2.

There are obvious differences in the virus proliferation in cells infected with a single subtype of H1N1 or H3N2 and in their co-infected cells (Fig. 4). In single-virus infected cells, both subtypes show an exponential increase, and the subtype H1N1 showed superiority to the H3N2 subtype during the late stage (Fig. 4a). In co-infected cells, the coinfection of H1N1 and H3N2 resulted in a dramatic decrease in the replication of H3N2 (Fig. 4b). This phenomenon may be associated with the activity of viral polymerases or other factors, suggesting that there is a complex interaction mechanism when these two viral strains are present in a single infected cell [2].

Simultaneous detection of multiple virus subtypes

Since different virus-specific MAbs can be coupled to different QD-SpA complexes and these can then be combined to create custom QD-SpA-MAb sets for the detection of specific combinations of viruses, we applied this technique

for the simultaneous detection of the three influenza A virus subtypes H1N1, H2N3 and H9N2 in infected MDCK cells. As shown in Fig. 5, by using the one-step staining procedure with a cocktail of QD625-SpA-MAb, QD525-SpA-MAb and QD705-SpA-MAb probes, the three influenza A virus subtypes H1N1, H3N2 and H9N2 were detected in the same co-infected MDCK cells with three types of corresponding QD signals (Fig. 5a). When the MDCK cells were co-infected with two types of influenza A virus subtypes, the two types of corresponding QD signals were detected (Fig. 5b). If there is only one type of virus subtype, only one corresponding QD signal can be detected (Fig. 5c). Interestingly, no cross-talk and no co-localization were observed between the different probes within the staining cocktail, indicating that each QD-SpA-MAb probe was uniquely matched to a specific target. This result is in agreement with the previous report that the HA protein is subtype-specific and hence can be used to detect specific subtypes of influenza virus [22]. It is also worth emphasizing that these results suggest the usefulness of QD-SpA-MAb probes for the simultaneous identification and differentiation of multiple virus subtypes.

Many studies have demonstrated the possibility of natural coinfection occurring with different subtypes of influenza viruses in humans, which may increase the opportunities for the occurrence of viral genetic reassortment within the human respiratory tract [23]. With our method, to detect coinfection by different subtypes of influenza viruses, only the Abs in the QD-SpA probe need to be replaced with highly specific MAbs for different subtypes. This makes the QD-SpA-MAb probes the most versatile assay for simple and sensitive virus detection compared with the other methods for the detection of coinfection. For example, traditional direct antigen detection tests, including enzyme immunoassays and direct fluorescent-antibody assays, suffer from poor sensitivity. The viral culture test is time-consuming and often not applicable [24, 25]. Likewise, serology to detect antibody response to infection may only produce positive results up to two weeks after

Fig. 5 Simultaneous detection of three influenza virus subtypes in infected MDCK cells. **a** Three colours were acquired by QD625-SpA-MAb, QD525-SpA-MAb and QD705-SpA-MAb probes from MDCK cells co-infected with H1N1, H9N2 and H3N2, respectively. **b** Two colours were acquired with the above group-specific probes when MDCK cells were co-infected with two subtypes. **c** A single colour was obtained from MDCK cells infected by one subtype. **d** No signal in non-infected cells. Scale bar, 10 μm
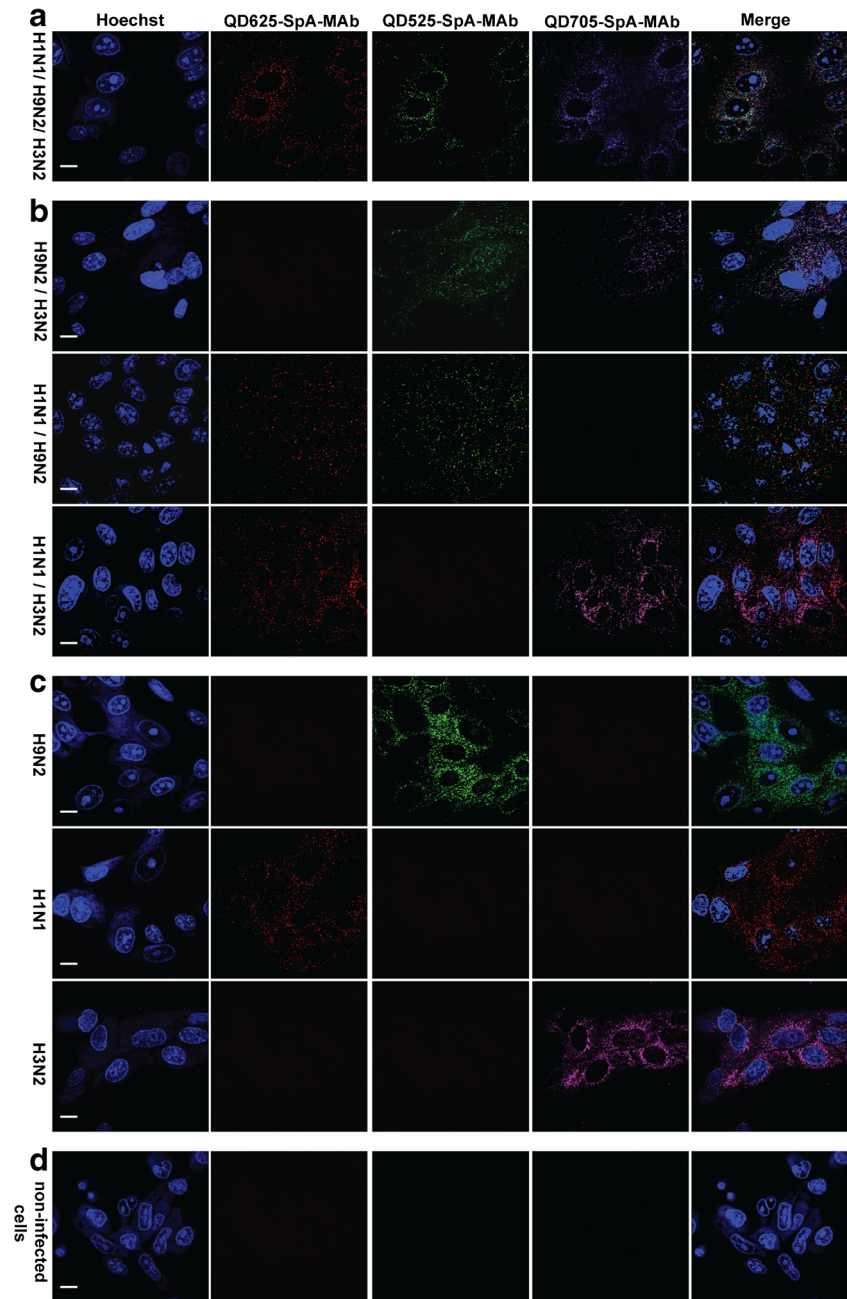
infection [26]. The PCR method can raise the false negativity if there is a mutation of the target site [27], or it may be caused by a mismatch between the primer and/or probe and its binding region [28]. Some more advanced methods, such as multiplex PCR, often produce false positive bands due to cross dimers forming between PCR primers [29].

### Simultaneous detection of viruses of different types

Then, the method was tested for the simultaneous detection of the co-infection of viruses of different types. Two probes, QD625-SpA-MAb and QD525-SpA-Mab, targeting HA and hexon proteins, respectively, were used in the A549

cell line co-infected with influenza A/H1N1 and HAdV-B3. As shown in Fig. 6, the results indicated that H1N1 and HAdV-B3 can be simultaneously stained with red and green signals by the two specific probes (Fig. 6a). When the cells were only infected with H1N1 or HAdV-B3, only the red or green signal can be detected (Fig. 6b, c), whereas no signal was found in the A549 cells without infection by of H1N1 or HAdV-B3 (Fig. 6d). This result further verifies that the QD-SpA-MAb probes are quite specific and can be effectively used for the simultaneous detection of coinfection with viruses of different types.

In the human respiratory tract, many coinfections of influenza with other viral agents, including HAdVs,

Fig. 6 Simultaneous detection of coinfection of H1N1 and HAdV-B3 (**a**) QD625-SpA-MAb and QD525-SpA-MAb probes simultaneously detected their targeted HA and hexon in A549 cells co-infected with H1N1 and HAdV-B3 viruses. **b** Only QD625-SpA-MAb targeting HA showed a signal in A549 cells infected with the H1N1 virus. **c** Only QD525-SpA-MAb probes targeting the hexon showed a signal in A549 cells infected with the HAdV-B3 virus. **d** There is no fluorescent signal in non-virus-infected cells. Scale bar, 10 μm
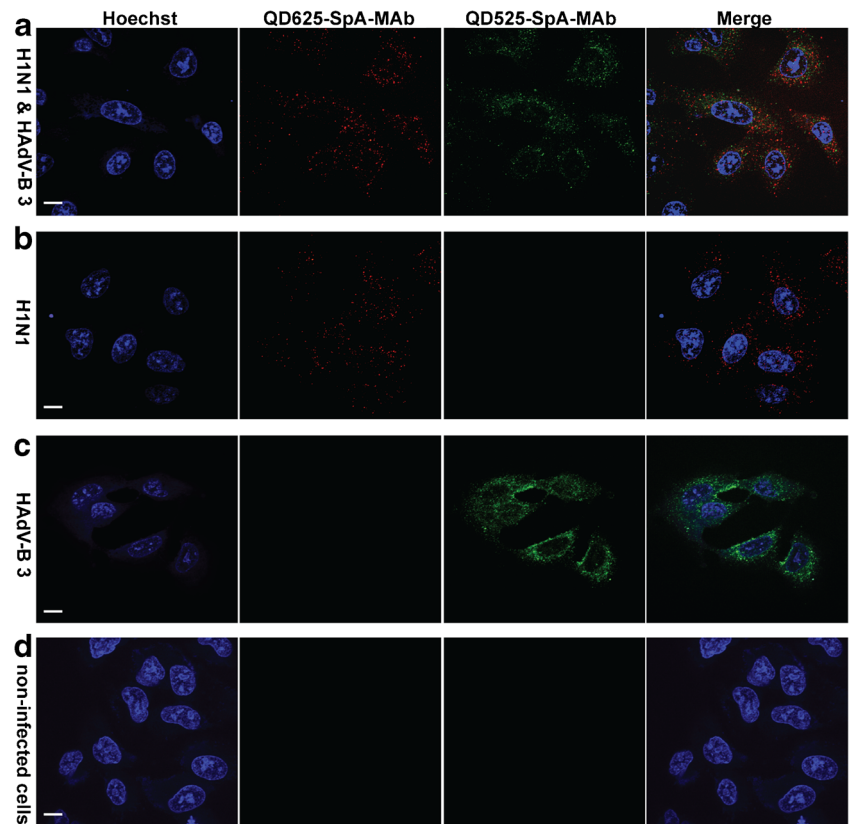
rhinovirus and coronavirus, have been reported [28]. The coinfection of novel influenza A/H1N1 virus and high severity HAdVs may cause progressive severe pneumonia [30]. Thus, our study provides a useful method for the detection of coinfection with viruses of different types.

Conclusion

In conclusion, we have imaged and analysed multiple viruses in cells by using multicolour quantum dot-based probes. The preparation procedure for these QD-SpA-MAb probes is a rapid, self-assembly and purification-free process. Within a single staining cycle, by using a cocktail of different coloured QD-SpA-MAb probes, multiple viruses in the same cell can be simultaneously imaged and analysed. Compared to other nanomaterials-based methods such as AuNPs/Ag staining [31], magnetic beads [32, 33], etc., the self-assembled QD-based method is flexible, sensitive, quantitative and prominent for multiple analysis, and thus is preferable for the co-infection detection in cell or tissue samples. Because one QD particle can be seen under microscope, the self-assembled quantum dot probes may be used to detect single targets of a virus. Of course, when the self-assembled quantum dot probes are used for virus detection, a protocol similar to that of immunofluorescence must be deployed. The differentiation ability of the new method also depends heavily on

the antibody. For example, in our experiment, we can't differentiate HAdV subtypes because antibodies specifically for different HAdV subtypes are unavailable. Moreover, the antigenicity of the sample needs to be preserved for detection. Nevertheless, our study provides a platform to perform the simultaneous detection of multiple viruses in the same cell.

As a whole, this approach may be useful in multiplexed applications for detecting and differentiating various viruses in the same infected cell or in the complex samples. Furthermore, QD-SpA-MAb probes able to diagnose the virus itself as well as its individual components due to its narrow band molecular spectra. This procedure consists of uncomplicated steps that do not require specialized skills or expertise in nanoparticles technology. The method can also provide information about the viral subcellular localization and quantitative evaluation for viral proliferation and replication, which may offer new opportunities for the molecular diagnosis of viruses and virus-cell interaction studies.

Compliance with ethical standards The author(s) declare that they have no competing interests.

References

1. Zhang W, Zhu D, Tian D et al (2015) Co-infection with avian (H7N9) and pandemic (H1N1) 2009 influenza viruses, China. Emerg Infect Dis 21:715–718
2. Ju L, Jiang L, Yang J et al (2010) Co-infection with influenza a/ H1N1 and a/H3N2 viruses in a patient with influenza-like illness during the winter/spring of 2008 in shanghai, China. J Med Virol 82:1299–1305
3. Wu W, Tang YW (2009) Emerging molecular assays for detection and characterization of respiratory viruses. Clin Lab Med 29:673–693
4. Jartti T, derlund-Venermo M, Hedman K et al (2013) New molecular virus detection methods and their clinical value in lower respiratory tract infections in children. Paediatr Respir Rev 14:38–45
5. Liotta LA, Kohn EC (2001) The microenvironment of the tumour-host interface. Nature 411:375–379
6. Bui VN, Ogawa H, Ngo LH et al (2013) H5N1 highly pathogenic avian influenza virus isolated from conjunctiva of a whooper swan with neurological signs. Arch Virol 158:451–455
7. Gao JH, Xu B (2009) Applications of nanomaterials inside cells. Nano Today 4:37–51
8. Zhao M, Zeng E (2015) Application of functional quantum dot nanoparticles as fluorescence probes in cell labeling and tumor diagnostic imaging. Nanoscale Res Lett 10:171
9. Zrazhevskiy P, True D, Gao X (2013) Multicolor multicycle molecular profiling (M3P) with quantum dots for single-cell analysis. Nat Protoc 8:1852–1869
10. Robertson JS, Cook P, Attwell AM, Williams SP (1995) Replicative advantage in tissue culture of egg-adapted influenza virus over tissue-culture derived virus: implications for vaccine manufacture. Vaccine 13:1583–1588
11. Huang X, Bronstein LM, Retrum J et al (2007) Self-assembled virus-like particles with magnetic cores. Nano Lett 7:2407–2416
12. Xing Y, Chaudry Q, Shen C et al (2007) Bioconjugated quantum dots for multiplexed and quantitative immunohistochemistry. Nat Protoc 2:1152–1165
13. Hanson DC, Schumaker VN (1984) A model for the formation and interconversion of protein A-immunoglobulin G soluble complexes. J Immunol 132:1397–1409
14. Xiong LH, Cui R, Zhang Z-L et al (2014) Uniform fluorescent Nanobioprobes for pathogen detection. ACS Nano 8:5116–5124
15. Zrazhevskiy P, Gao X (2013) Quantum dot imaging platform for single-cell molecular profiling. Nat Commun 4:1619
16. Wu F, Yuan H, Zhou C et al (2016) Multiplexed detection of influenza a virus subtype H5 and H9 via quantum dot-based immunoassay. Biosens Bioelectron 77:464–470
17. Atkins L, Burman D, Chamberlain S et al (2008) S. aureus IgG-binding proteins SpA and Sbi: host specificity and mechanisms of immune complex formation. Mol Immunol 45:1600–1611
18. Moks T, Abrahmsén L, Nilsson B et al (1986) Staphylococcal protein a consists of five IgG-binding domains. Eur J Biochem 156: 637–643
19. Guarner J, Shieh WJ, Dawson J et al (2000) Immunohistochemical and in situ hybridization studies of influenza a virus infection in human lungs. Am J Clin Pathol 114:227–233
20. Sohn S-Y, Hearing P (2016) Adenovirus early proteins and host sumoylation. mBio 7(5):e01154–e01116
21. Smith JG, Wiethoff CM, Stewart PL, Nemerow GR (2010) Adenovirus. J Microbiol Immunol 343:195–224
22. Detmer S, Gramer M, Goyal S et al (2013) Diagnostics and surveillance for swine influenza. J Microbiol Immunol 370:85–112
23. Claas EC, Kawaoka Y, de-Jong JC et al (1994) Infection of children with avian-human reassortant influenza a virus from pigs in Europe. J Virol 204:453–457
24. Ginocchio C, Zhang F, Manji R et al (2009) Evaluation of multiple test methods for the detection of the novel 2009 influenza a (H1N1) during the new York City outbreak. J Clin Virol 45:191–195
25. Kim D, Poudel B (2013) Tools to detect influenza virus. Yonsei Med J 54:560–566
26. Tanner H, Boxall E, Osman H (2012) Respiratory viral infections during the 2009–2010 winter season in Central England, UK: incidence and patterns of multiple virus co-infections. Eur J Clin Microbiol Infect Dis 31:3001–3006
27. Zheng X, Todd KM, Yen-Lieberman B et al (2010) Unique finding of a 2009 H1N1 influenza virus-positive clinical sample suggests matrix gene sequence variation. J Clin Microbiol 48:665–666
28. Cho CH, Lee CK, Nam M-H et al (2014) Evaluation of the AdvanSure™ real-time RT-PCR compared with culture and Seeplex RV15 for simultaneous detection of respiratory viruses. Diagn Microbiol Infect Dis 79:14–18
29. Zhang G, Hu Y, Wang H et al (2012) High incidence of multiple viral infections identified in upper respiratory tract infected children under three years of age in shanghai, China. PLoS One 7:e44568
30. Lee MJ, Cheng I, Chen Y-L et al (2012) Co-infection of infleuenza a and adenovirus in an infant. J Pediatr Resp Dis 8:123–127
31. Tsang M-K, Ye W, Wang G et al (2016) Ultrasensitive detection of Ebola virus oligonucleotide based on Upconversion Nanoprobe/ Nanoporous membrane system. ACS Nano 10:598
32. Zhang R-Q, Liu S-L, Zhao W et al (2013) A simple point-of-care microfluidic Immunomagnetic fluorescence assay for pathogens. Anal Chem 85:2645–2651
33. Wu Z, Hu J, Zeng T et al (2017) Ultrasensitive Ebola virus detection based on electroluminescent Nanospheres and Immunomagnetic separation. Anal Chem 89:2039–2048